

Wind Turbine and Grid Interaction Studies Using Integrated Real-Time Simulation Environment

A. Mäkinen, H. Tuusa

Abstract—Knowledge of interactions between wind turbines and network becomes essential as the number of wind turbines installed in the network increases. Thus, a simulation environment with accurate network and wind turbine models is needed. In this paper, a novel real-time simulation environment for wind turbine and grid interaction studies is presented. The network is simulated with Real-Time Digital Simulator (RTDS) and the wind turbine with its power electronic equipments in dSPACE. First, the wind turbine model is introduced. Next, real-time simulation results during three-phase short-circuit and automatic reclosing are presented and compared to Simulink results in order to verify the real-time model. Discussions about the reliability and usefulness of the environment are also performed.

Index Terms—Real-time simulation environment, RTDS, dSPACE, Permanent magnet synchronous generator (PMSG), Voltage source converter, LCL-filter, three-phase short-circuit.

I. INTRODUCTION

In the future, wind power will be a remarkable power source because of its environment friendliness. According to the WWEA (World Wind Energy Association), 19 696 MW of new wind energy capacity were added in the year 2007 and by the end of December 2007, the global wind energy capacity had increased to 93 849 MW. This means that wind turbines already generate more than 1 % of the total electricity in the world. [1]

However, wind turbines affect the power system differently than the synchronous generators used in conventional power plants. Therefore, interactions between the wind turbines and the utility grid have to be well-known. [2][3][4] In this paper, an integrated real-time simulation environment is introduced. A wind power system is also modeled and simulated during a three-phase short circuit. In addition, the reliability of the real-time simulations is assessed.

The integrated real-time simulation environment constructed using Real-Time Digital Simulator (RTDS) and dSPACE enables the use of accurate wind turbine and network models. Further, the simulation environment used makes it possible to develop control strategies for wind turbines to qualify more demanding grid codes in the future.

Main contact: Anssi Mäkinen, Department of Electrical Energy Engineering, Tampere University of Technology, Finland.
e-mail: anssi.makinen@tut.fi, fax: +358331152369.

Minimization of the simulation time and the possibility to share calculation power between two simulators can be considered as additional benefits. The aforementioned environmental properties enable simulations of more complex models. In addition, it is possible to use real devices e.g. protection relays, as a part of a simulation system.

Integrated real-time simulation environment of RTDS and dSPACE has been studied earlier e.g. in [5], [6] and [7]. The environment was tested for active power filtering studies in [5]. In [6] the environment was used to study grid impacts of distributed generation. However, simulation results were presented and analyzed only from the power systems point of view. In [7], a wind turbine model was implemented in RTDS, while dSPACE was used to provide wind velocity profiles for test. This paper extends the analysis to cover the behavior of the wind turbine, not only the power system as in [6].

II. REAL-TIME SIMULATION ENVIRONMENT

The real-time simulation environment consists of two simulators, dSPACE and RTDS, and two computers, which are used to control the simulators. The simulators communicate through analog area implemented using D/A and A/D converters. Figure 1 shows the practical implementation of the real-time simulation system.

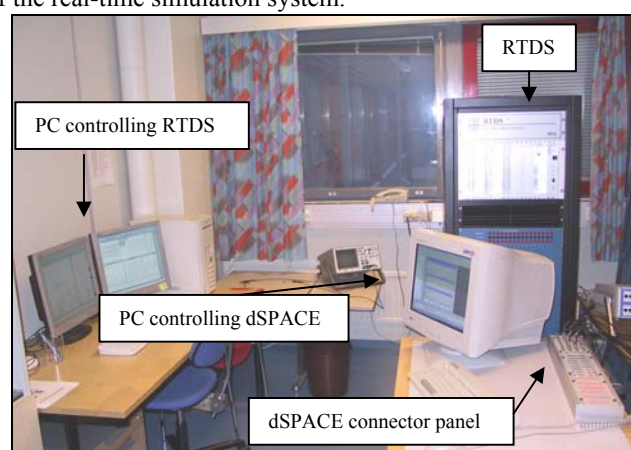


Fig. 1. Practical implementation of the real-time simulation environment. [6]

A. RTDS

RTDS is a digital electromagnetic transient power system simulator. The hardware of RTDS consists of parallel processor cards placed on modular units called racks. If more

calculation power is needed, extra processors can be connected to the rack or new racks can be installed. The signals from the outside can be transferred to the system via digital and analog I/O channels.

The software that controls the RTDS simulation is called RSCAD. The system modeling is performed in Draft mode, which contains a library of power and control system component models. The controlling and observing of simulations is performed in RSCAD's Runtime-mode. It is possible to create different kinds of fault situations such as short circuits, connections of heavy loads or breaker openings that create an unwanted islanding. Figure 2 represents the user interface of the Runtime mode. [8]

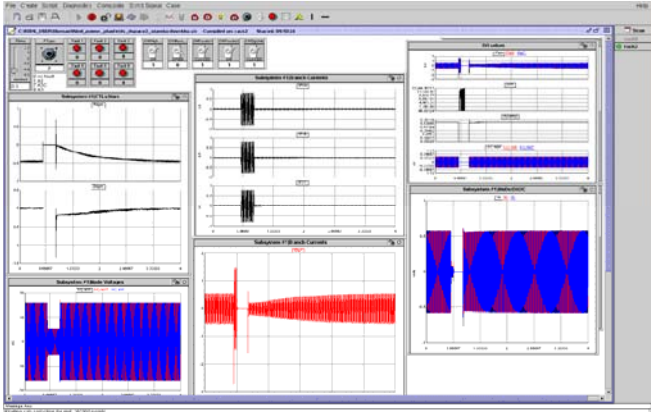


Fig. 2. The user interface of the Runtime-mode of the RSCAD.

B. dSPACE

dSPACE DS1103 PPC Controller Board is specifically designed for test and development of high-speed multivariable digital controllers and for real-time simulations in various fields. The hardware consists of a Power PC processor and an additional DSP controller. In addition, there are number of interfaces containing digital I/O channels, A/D and D/A channels, CAN, serial and incremental encoder interfaces. A Connector panel shown in Fig. 3 is used to connect external I/O signals to the dSPACE processor card. The software used to control dSPACE simulations is called ControlDesk shown in Fig. 4. ControlDesk allows management of the simulation by providing a virtual control panel with online parameter changing and scopes. [9]



Fig. 3. dSPACE connector panel CLP 1103. [5]

Matlab equipped with Simulink and Real-Time Workshop software enable the use of dSPACE. The connections between Matlab/Simulink and dSPACE are shown in Fig. 5. First, the control system is modeled in Simulink. Next, the model is translated into C-code with the help of Real-Time Workshop.

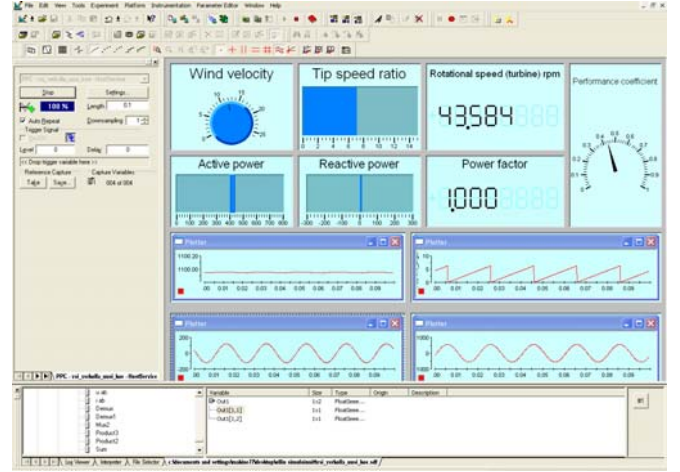


Fig. 4. ControlDesk program for controlling the dSPACE simulation.

The function of the C-compiler is to make the code suitable for dSPACE hardware. The simulation is controlled using ControlDesk.

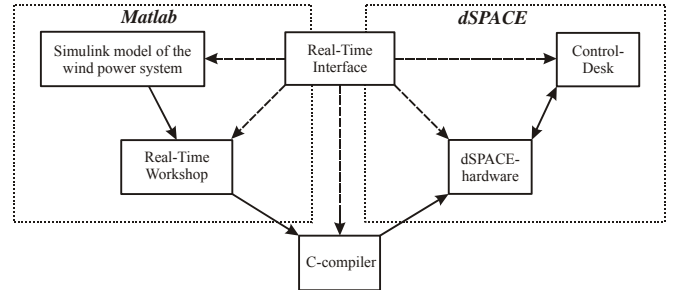


Fig. 5. The development process of the dSPACE model.

III. SYSTEM MODELING

Figure 6 illustrates the modeled space-vector based wind power system. The rotor extracts kinetic energy from the wind and converts it into rotational energy of the rotor shaft. The gearbox between the rotor and the generator is used to increase the rotational speed of the shaft in order to be more suitable for the generator. The permanent magnet synchronous generator (PMSG) is connected to the grid through a back-to-back voltage source converter. The generator side converter controls the generator torque and the rotor shaft speed. The function of the grid side converter is to control the active and reactive power, which is transferred to the grid via an LCL-filter. An ideal step-up transformer is used to match the voltage level to the medium voltage network, which consists of RL-load, two wires in medium voltage level and grid.

A. Rotor and Gearbox

The wind turbine model is based on the following equation: [10]

$$T_t = \frac{P_t}{\omega_t} = \frac{c_p(\lambda, \theta) \rho A v^3}{2\omega_t} \quad (1)$$

where T_t , P_t , c_p , λ , θ , ρ , ω_t , A and v corresponds to the torque produced by the wind turbine, active power produced, performance coefficient, tip speed ratio, pitch angle of the rotor, air density, angular speed of the rotor, swept area, and

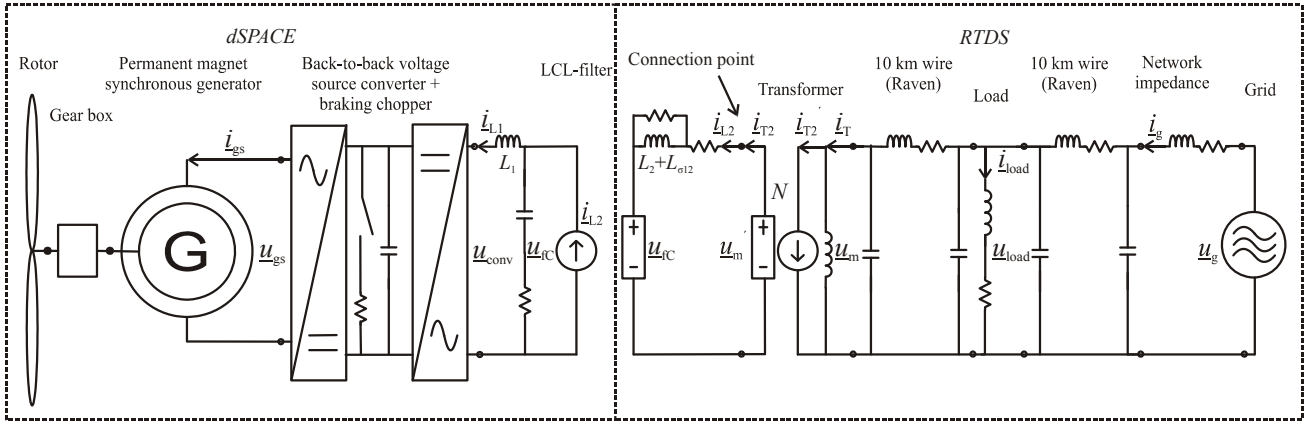


Fig. 6. Modelled wind power system

wind speed respectively. The ideal gearbox is modeled using transmission ratio n :

$$n = \frac{\omega_g}{\omega_t} = \frac{T_t}{T_g} \quad (2)$$

where ω_g corresponds to the angular speed of the generator rotor and T_g is the torque extracted from the wind reduced to the generator shaft. The rotational system is modeled based on the equation of motion: [10]

$$J \frac{d\omega_g}{dt} = T_g - T_e - B\omega_g \quad (3)$$

where J is the total inertia of the wind turbine system and B is constant that takes the fraction losses into account.

B. PMSG

Traditionally, synchronous generators are excited with DC-current fed to the rotor windings. [11] In case of PMSG, rotor windings are replaced by permanent magnets providing a much simpler structure for the generator. [12] The copper losses are reduced because there are no current circuits in the rotor. Additionally, the efficiency is increased as the excitation is executed without any energy supply. The maintenance costs are also reduced since the slip rings for the excitation current can be omitted. [11][12]

However, permanent magnets are very expensive and difficult to handle during manufacturing. Also, it might be difficult to keep the operating temperature of the magnets cooler than the Curie point of the magnet, i.e., the maximum temperature at which the magnet loses its magnetic qualities. [13]

The PMSG used in this study is modeled in a rotor reference frame. The voltage equations of the PMSG in the rotor reference frame can be expressed as follows: [14]

$$\begin{aligned} u_{gs,d} &= R_s i_{gs,d} + \frac{d\psi_d}{dt} - \omega_g \psi_q \\ u_{gs,q} &= R_s i_{gs,q} + \frac{d\psi_q}{dt} + \omega_g \psi_d \end{aligned} \quad (4)$$

where $u_{gs,d}$ and $u_{gs,q}$ are the terminal stator voltages, $i_{gs,d}$ and $i_{gs,q}$ are the stator currents and ψ_d and ψ_q are the stator flux linkages. The stator flux linkages are: [14]

$$\psi_{gs,d} = L_d i_{gs,d} + \psi_m \quad (5)$$

$$\psi_{gs,q} = L_q i_{gs,q}$$

where L_d and L_q are inductances and ψ_m is the permanent magnet flux linkage. The electrical torque T_e is calculated based on the following equation: [14]

$$T_e = \frac{3}{2} p (\psi_m i_{gs,q} + i_{gs,q} i_{gs,d} (L_d - L_q)) \quad (6)$$

where p is a number of pole pairs.

C. Voltage Source Converter

A voltage source converter connected to the stator of the PMSG effectively decouples the generator from the network. Thus, the generator rotor and the wind turbine rotor can rotate freely depending on the wind conditions. In the system modeled, the electrical energy from the generator is rectified to a dc link with help of active generator side converter. Then, the grid side converter converts the dc voltage to 50 Hz ac voltage. The braking chopper is modeled in the dc-link in order to protect the dc-link capacitor during fault situation. The chopper is activated when the dc link voltage increases over the predefined limit. Such a situation may arise, for instance, during voltage dip in the grid when all energy generated from the wind cannot be transferred to the grid.

There are several reasons promoting the use of active generator side converter. The stator current of the PMSG can be controlled to be sinusoidal. Under nominal wind speed the rotational speed of the wind turbine can be controlled to operate with maximum performance coefficient. In other words, the energy extracted from the wind is maximized. Additionally, during grid fault, the torque of the generator can be decreased so that the imbalance between generated power by the generator and transferred power to the grid reduces, which restrains the rising of the dc-link voltage. Thus, the low voltage ride through, which is considered to be the main challenge to wind turbine manufacturers [3], becomes easier to implement. [11][14]

The modeled frequency converter is assumed to be ideal.

$$P_{ac} = P_{dc} \quad (7)$$

Thus,

$$\frac{3}{2}(u_{gs,d}i_{gs,d} + u_{gs,q}i_{gs,q}) = u_{dc}i_{dc,g} \quad (8)$$

$$\frac{3}{2}(u_{conv,d}i_{L1,d} + u_{conv,q}i_{L1,q}) = u_{dc}i_{dc,c}$$

where u_{dc} is the dc-link voltage, $i_{dc,g}$ and $i_{dc,c}$ are the generator and grid side dc currents, u_{conv} is the grid side converter voltage and i_{L1} is the grid side converter current.

Both the generator and the grid side converters are assumed to execute their voltage reference ideally. In other words, the modulators are not modeled. This is due to the fact that the calculation power of the real-time simulators is not sufficient to execute the real time simulation with such a small simulation step-size. However, harmonics and switching performance of the frequency converter are not essential in this analysis and, on the other hand, if there is a need to examine phenomena around the switching frequency, Simulink offers powerful and reliable tool for this purpose.

D. LCL-Filter

Modulation of power electronic converters causes current harmonics around the switching frequency which can disturb sensitive devices on the grid. In addition, harmonics produce extra losses. One possible solution for dampening the switching ripple current is to use an LCL-filter. The LCL-filter is a third-order low-pass filter, which has a great harmonic performance at low switching frequencies. Thus, this filter type is very attractive for high power applications. However, if the LCL-filter is not properly designed, harmful resonances may occur due to the converter current or network voltage harmonics. Therefore the filter should be damped.[15]

The size of the magnetic material is kept to a minimum since it directly affects the filter overall costs. Such a design increases the filter capacitance needed to obtain the desired resonance frequency. However, the function of the converter side inductor is to attenuate the converter switching ripple current enough so the size of the inductor cannot be reduced without restrictions. Another constraining factor is the amount of reactive power of the filter produced, which increases as the filter capacitance increases. [16] Usually, the size of the grid side inductor is much smaller than the converter side inductor. The size of the grid side inductor affects to the filter's resonance frequency.

In the simulation model, the inductance of the grid side inductor corresponds to the sum of the grid side filter inductance L_2 and the leakage inductance of the transformer $L_{12\sigma}$, as shown in Fig. 6. In addition, the grid side inductor is modeled with first-order Foster circuit to take into account the frequency dependence of the inductor in order to give more accurate inductor model. [17] In addition, the Foster circuit effectively attenuates the noise arising during data transmission in RTDS/dSPACE environment. The damping of the filter is done by connecting the damping resistances in series with the filter capacitors. [15]

In the model, the RMS value of the current in switching frequency is not allowed to be higher than 20 % of the

fundamental frequency current. The size of the grid side inductor is determined using the index r that describes the relation between the two inductances: [15]

$$L_1 r = (L_2 + L_{L12\sigma}). \quad (9)$$

The value for the r is chosen to be 1/3 and L_1 are the inductance of the converter side inductor. The resonance frequency is chosen to be 500 Hz.

E. Transformer and Network

In the model, the wind turbine is connected to the voltage level of 20 kV using an ideal step-up transformer. The transformation ratio N is defined as follows: [18]

$$N = \frac{u_m}{\underline{u}_m} \quad (10)$$

Thus, the secondary side current i_{T2} can be reduced to the primary side of the transformer as follows: [18]

$$i_{T2}' = \frac{1}{N} i_{T2} \quad (11)$$

The wires of the medium voltage network have been modeled with π -model consisting of a series resistance, a series inductance and two parallel capacitors. The wire type is Raven, which is often used in medium voltage networks. The RL-load is assumed to be passive. The nominal values of the load are $P=1000$ kW and $\cos \varphi= 0,95$. The grid is modeled as a voltage source behind the impedance.

F. Generator Side Converter Control

The control system used in the generator side converter is based on vector control in rotor reference frame. The generator side converter is controlled to extract the maximum power from the wind under nominal wind speed that is used in the simulation. The control system is presented in Fig. 7. The inner loop of the control system controls the stator current (torque) of the PMSG and the outer loop controls the angular speed of the PMSG rotor.

The speed reference is compared to the measured speed. The speed error is inputted to the PI-controller, giving the quadrature axis current reference as output. The current reference $i_{gs,q}^*$ is compared to the actual measured current $i_{gs,q}$. The current error is then fed into another PI-controller. The direct axis current reference is $i_{gs,d}^*$ is set to zero in order to simplify the control strategy. The reference value is compared to the measured value $i_{gs,d}$ and the current error is fed to the current controller.

In order to control the currents $i_{gs,d}$ and $i_{gs,q}$ independently, the cross-coupling effect is removed by adding the compensation terms $\omega_g L_q i_{gs,q}$ and $\omega_g (\psi_m + L_d i_{gs,d})$ to the outputs of the d and q axis current controllers. As a result, the reference value of the stator voltage vector \underline{u}_{gs}^* is obtained. [12]

G. Grid Side Converter Control

The aim of the grid side converter control is to keep the dc link voltage constant, thereby ensuring that the active power generated by the generator is fed to the network. Additionally,

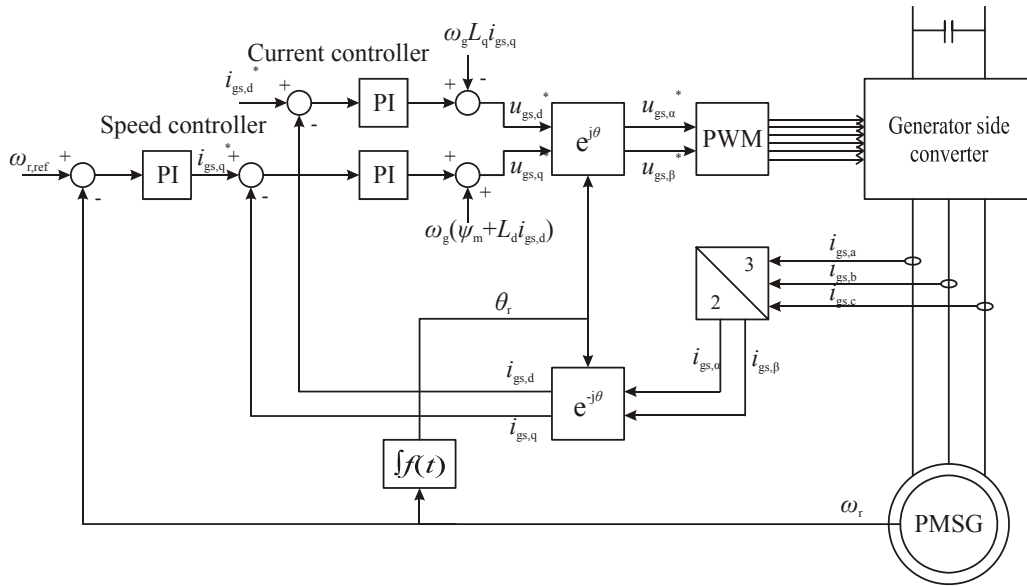


Fig. 7. Control of the generator side converter.

it is possible to control the reactive power fed to the grid.

The grid side converter is controlled in a synchronous reference frame that rotates synchronously with the connection point voltage vector $\underline{u}_{\text{sync}}$, which corresponds to the voltage vector \underline{u}_m' shown in Fig. 6. The phase angle of the fundamental frequency component of the connection point voltage is extracted using phase-locked loop (PLL). The control strategy is implemented, similarly as in the case of generator side converter, with two cascade loops. The fast inner loop controls the grid current i_{L1} and the outer loop controls the dc link voltage u_{dc} . The control system is presented in Fig. 8.

The dc link voltage reference u_{dc}^* is compared to the actual measured voltage u_{dc} . The dc-link voltage error is fed to the PI-controller as an input and a direct axis current reference

$i_{L1,d}^*$ is obtained. The current reference of the d-axis component is then compared to the measured current $i_{L1,d}$ and the error current is fed to the current PI-controller. [4]

The reactive power transferred to the network can be regulated with the quadrature axis current component $i_{L1,q}$. The target of the reactive power control is, in this case, to produce unity power factor to the connection point of the wind turbine system. The unity power factor in connection point is achieved when $i_{L2,q}$ is zero. Thus, the current flow through a filter capacitor must be taken into account. [15] In the paper, the value for the reference current $i_{L1,q}^*$ is determined empirically with the help of iterative simulations.

The reference current $i_{L1,q}^*$ is compared to measured current $i_{L1,q}$ and the current error is fed to the current PI-controller. The output of the current controller is the reference voltage

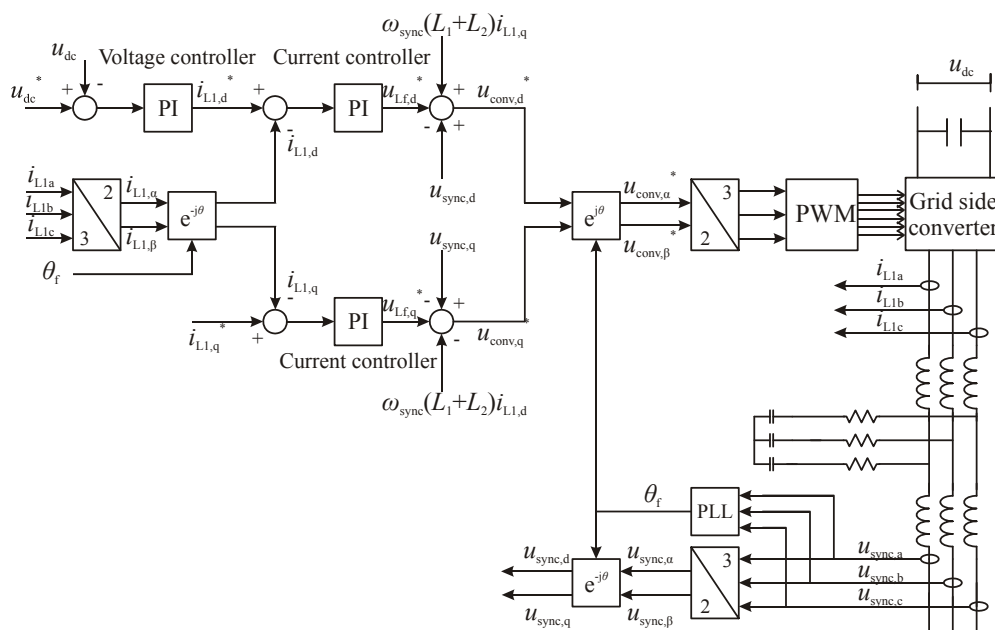


Fig. 8. Control of grid side converter.

over the two filter inductors \underline{u}_{Lf}^* . Removing the cross-coupling terms and with the help of the measured connection point voltage \underline{u}_{sync} , the converter voltage reference \underline{u}_{conv}^* can be presented.

IV. SYSTEM SIMULATION IN RTDS/dSPACE ENVIRONMENT

Figure 9 presents the block diagram of the RTDS/dSPACE implementation. First, the wind turbine and the back-to-back voltage source converter are modeled in Simulink. Next, the model is compiled to C-code and uploaded to dSPACE. The real-time simulation is controlled and observed from a PC with the ControlDesk.

The network is modeled in RSCAD Draft mode. Based on the model, the RTDS makes the real-time simulation, which in turn can be controlled and observed in the Runtime mode of RSCAD. In the case studied, dSPACE receives connection point voltage $u_{m(a,b,c)}$ and connection point current $i_{L2(a,b,c)}$ from the RTDS and gives back the voltage over the LCL-filter capacitor $u_{fc(a,b,c)}$ to RTDS. In other words, the wind turbine system modeled in dSPACE is a voltage source in the RTDS. Data transmission between the simulators is done via analog signals.

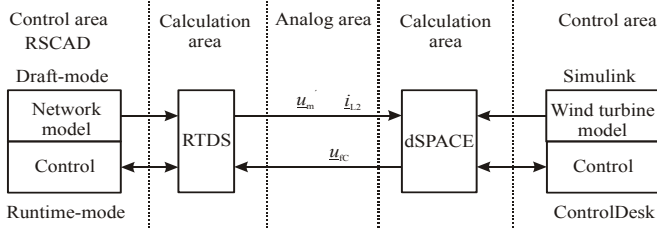


Fig. 9. System modeling in RTDS/dSPACE environment.

V. SIMULATION CASE

As an example of the behavior of the simulation environment a wind turbine system presented in Fig. 6 is modeled and simulated during a three-phase short-circuit, which occurs on the high-voltage side of the transformer. In the integrated real-time simulation environment, the wind turbine with its power electronic equipment is simulated in dSPACE and the network in RTDS. Same system is also simulated in Matlab/Simulink to verify the real-time simulation model. Simulation in Matlab/Simulink is carried out using smaller simulation step-size (10 μ s) in order to achieve accurate reference results. The simulation step-size used in dSPACE is 100 μ s and in RTDS the step-size is 50 μ s. The wind speed is assumed to be constant, 12 m/s, during the simulation. The system parameters are shown in Table 1.

VI. SIMULATION RESULTS

The short-circuit occurs at time 419.954 s and automatic reclosing clears the fault in the feeder within 300 ms. After 50 ms from the beginning of the fault, the converter references for active and reactive power as well as the generator torque are switched to zero. Hence, the wind turbine does not disturb the automatic reclosing and the generator does not supply power to the dc-link.

TABLE I
SYSTEM PARAMETERS

air density $\rho = 1,25$ [kg/m ³]	rotor diameter = 37 [m]
gearbox transmission ratio $n = 10$	wind turbine system inertia
fraction term $B = 0,25$ [Nms/rad]	$J = 15$ [kNms ² /rad]
PMSG power $S = 500$ [kVA]	permanent magnet flux linkage
stator inductance $L_d = 0,83$ [mH]	$\psi_m = 2,29$ [Wb]
dc-link voltage $u_{dc} = 1100$ [V]	pole pairs $p = 6$
resonance frequency $f_{res} = 500$ [Hz]	stator inductance $L_q = 0,88$ [mH]
switching frequency $f_{sw} = 3000$ [Hz]	filter inductance $L_1 = 350$ [μ H]
filter inductance $L_2 + L_{12\sigma} = 108$ [μ H]	filter capacitor $C_f = 1,6$ [mF]
transformation ratio $N = 29$	

As a result of the short-circuit, the connection point voltage u_m' drops to zero, Fig. 10, and the converter starts to feed the fault current, Figs. 11, 12 and 13. The upper figures correspond to the Simulink and lower figures to the RTDS/dSPACE simulations respectively. Fig. 12 presents the transition to short-circuit of the converter current i_{L1} so the time scale of the figure is different than in other figures. The phase difference between currents shown in Fig. 12 occurs due to the fact that the drawing of the graphs cannot be started at the same time in dSPACE and Simulink. After the reference values for the active and reactive power are switched to zero, no current is transferred to the network.

When the fault is cleared, the converter reference values, which were switched to zero, are increased in a controlled manner. It can be seen from Figs. 11 and 13 that transients occur to the currents i_{L1} and i_{L2} as the connection point voltage u_m' returns. The transients of i_{L1} occur since the converter voltage is zero when the voltage comes back. The transients of i_{L2} can be reduced by increasing the value of the damping resistance of the LCL-filter. Although the same value of the damping resistance is used in both simulation environments, the transients are greater in RTDS/dSPACE. This is because of the longer simulation step-size and the delay between the two simulators.

Because of the zero voltage at the connection point during short-circuit no power can be transferred to the network, Fig. 14. Thus, the energy extracted from the wind is stored in the dc-link of the voltage source converter causing the dc-link voltage u_{dc} to increase as shown in Fig. 15. In the system modeled, the braking chopper, Fig. 16, is activated as the dc-link voltage reaches 1300 V and the power generated from the wind is dissipated in resistance. When the reference values of the converters are switched to zero, no power is transferred into the dc-link and, on the other hand, no power is transferred out of the dc-link. As a result, the dc-link voltage remains constant. After the network voltage returns, the dc-link voltage controller regulates the voltage u_{dc} back to its reference value. Also, the active power p is returned to its nominal value.

When the torque reference of the PMSG is set at zero, the kinetic energy from the wind is stored in the rotating mass of the wind turbine rotor. Thus, the rotational speed of the turbine is increased as shown in Fig. 17. The acceleration of the turbine speed continues as long as the mechanical torque of the rotor of the PMSG is greater than the electrical torque controlled by the generator side converter.

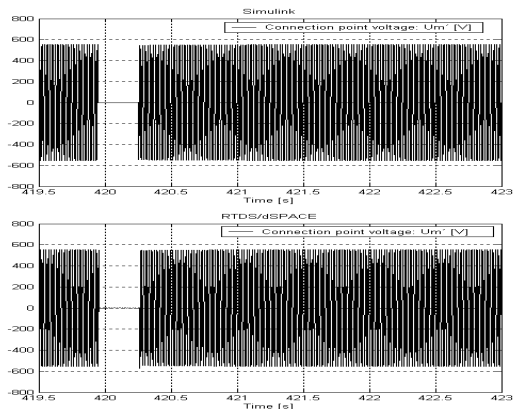


Fig. 10. Connection point voltage U_m' during three-phase short-circuit.

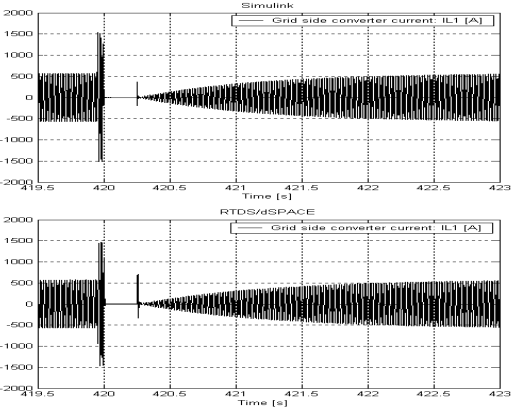


Fig. 11. Grid side converter current i_{L1} .

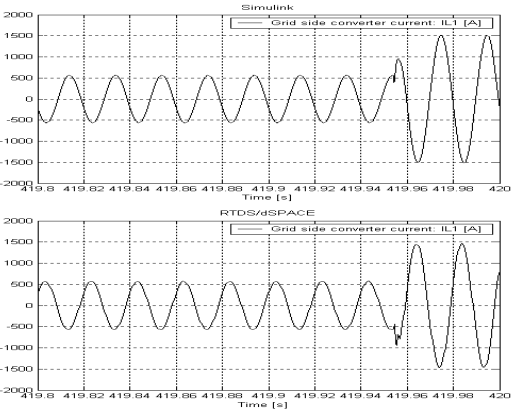


Fig. 12. Transient of the i_{L1} .

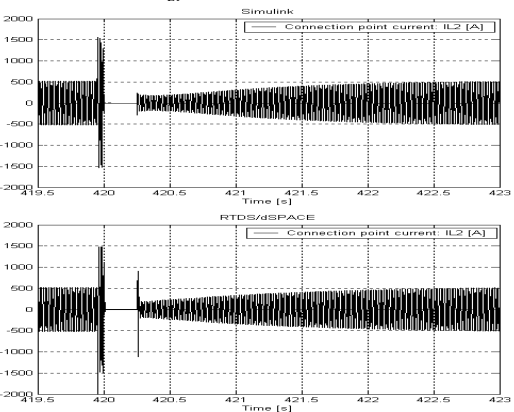


Fig. 13. Connection point current i_{L2} .

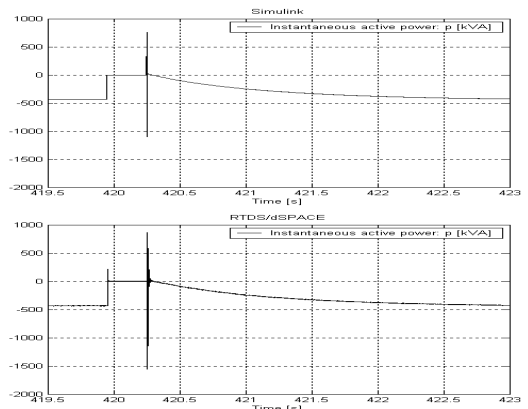


Fig. 14. Instantaneous active power p .

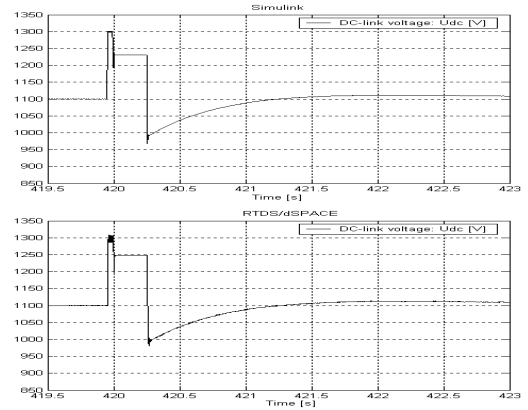


Fig. 15. DC-link voltage U_{dc} .

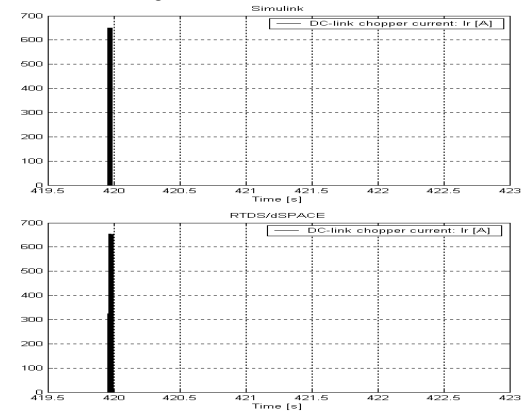


Fig. 16. DC-link chopper current i_r .

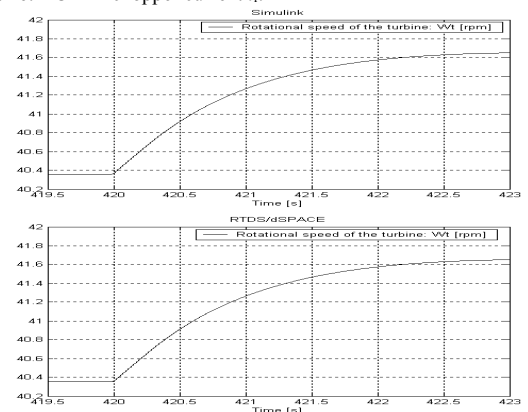


Fig. 17. Rotational speed of the wind turbine ω_t .

VII. DISCUSSION

In this paper, a variable-speed wind turbine connected to the medium voltage feeder was modeled in both RTDS/dSPACE and Simulink environments. The behavior of both simulation environments was simulated during automatic reclosing occurring because of short-circuit. The simulation results obtained were largely in agreement with each other during steady state operation. However, to achieve this kind of results, the delay between the real-time simulators must be compensated. In this study, the angle of the voltage vector \underline{u}_{FC} , which was fed from the dSPACE to RTDS, was manipulated to compensate the delay. The most congruent real-time simulation results compared to Simulink results were obtained when the value for the compensated delay was set at 400 μ s. The delay compensation method is effective during steady state or slowly varying mode of operation because the length of the voltage vector is fixed. However, problems occur during transient simulations because it is impossible to predict how the length of the vector will change. Therefore the delay compensation method used is not very effective in the case of transient simulation.

Another problem related to the real-time simulation environment is the asynchronous operation of the simulators, which causes varying delay. One possible way to avoid the problem is to feed an external interrupt signal from the RTDS to dSPACE to synchronize the calculations of the simulators. In preliminary simulations, it was possible to keep the delay successfully fixed but problems were encountered as a result of the limited calculation power of the dSPACE as the size of the wind turbine model with its frequency converter requires a great deal of calculation power.

Despite a few problems encountered in using the real-time environment, several major advantages make the environment attractive. As mentioned above, the simulation time is minimized. In this case, 430 second real-time simulation required simulation time of 4 hours and 28 minutes in Simulink. In addition, trimming of the control parameters of the PI-controllers and testing of the control algorithms during fault situations were much easier in the real time environment.

VIII. CONCLUSION

The simulation results show that the combination of RTDS and dSPACE are in great agreement with Simulink in continuous mode of operation. Transients in RTDS/dSPACE environment are greater because of longer simulation step-size (100 μ s in dSPACE and 50 μ s in RTDS) and the delay (\approx 400 μ s) between the simulators. In general, the simulation results show that differences between simulation environments are of no remarkable importance. As a conclusion to this study it can be stated that the real-time simulation environment is almost as reliable and useful tool for studies on interactions between wind turbines and network as Simulink, which requires much more simulation time. With the environment it is possible to test and improve e.g. control algorithms and protection mechanisms of wind turbine in fault

situations. The next step in the development of the real-time simulation environment is to measure data from the real wind power system and validate the model by comparing the simulated and measured results.

REFERENCES

- [1] WWEA (World Wind Energy Association) Website. April 2008. Available: <http://www.wwindea.org/home/index.php>.
- [2] Kling, W.L., Sloopweg, J.G. 2003. Wind Turbines as Power Plants. Electrical Power Systems Laboratory, Faculty of Information Technology and Systems, Delft University of Technology, Netherlands. 7 p.
- [3] Carrasco, J. M., Franquelo, L. G., Bialasiewicz, J. T., Galván, E., Guisado, R. C. P., Prats, M. Á. M., León, J. I., Moreno-Alfonso, N. 2006. Power-Electronic Systems for the Grid Integration of Renewable Energy Sources: A Survey. IEEE Transactions on Industrial Electronics, Vol. 53, No. 4, August 2006. pp. 1002 - 1016.
- [4] Blaabjerg, F., Teodorescu, R., Liserre, M., Timbus, A.V. 2006. Overview of Control and Grid Synchronization for Distributed Power Generation Systems. IEEE Transactions on Industrial Electronics, Vol. 53, No.5, October 2006, pp. 1398 - 1409.
- [5] Mäki, K., Partanen, A., Rauhala, T., Repo, S., Järventausta, P., Parkatti, P., Tuusa, H. 2006. Real-time environment for power system studies using RTDS and dSPACE simulators. NORPIE'06 Nordic Workshop on Power and Industrial Electronics, 12-14 June, 2006, Lund, Sweden 7 p.
- [6] Mäki, K., Kulmala, A., Repo, S., Järventausta, P. 2007. Studies on Grid Impacts of Distributed Generation in a Combined Real-Time Simulation Environment. 7th International Conference on Power System Transients, IPST 2007, 4-7 June, Lyon, France, 6 p.
- [7] Steurer, M., Li, S., Wooddruff, S., Shi, K., Zhang, D. 2004. Development of a Unified Design, Test, and Research Platform for Wind Energy Systems based on Hardware-In-the Loop Real Time Simulation. 35th Annual IEEE Power Electronics Specialists Conference, Aachen, Germany pp. 3604 - 3608.
- [8] RTDS Technologies, 2005. "Real-Time Digital Simulator Power System Users Manual".
- [9] Real-Time Interface (RTI and RTI-MP) Implementation Guide. 2004. dSPACE. 304 p.
- [10] Sun, T., Chen, Z., Blaabjerg, F. Voltage Recovery of Grid-Connected Wind Turbines with DFIG after a Short-Circuit Fault. 35th Annual IEEE Power Electronics Specialists Conference, 2004, Aachen Germany, pp. 1991 - 1997.
- [11] Hansen, L.H., Helle, L., Blaabjerg, F., Ritchie, E., Munk-Nielsen, S., Bindner, H., Sørensen, P., Bak-Jensen, B. Conceptual survey of Generators and Power Electronics for Wind Turbines. Risø-R-1205(EN), Risø National Laboratory, Roskilde, Denmark, December 2001, 108 p.
- [12] Eskola, M. 2006. Speed and Position Sensorless Control of Permanent Magnet Synchronous Motors in Matrix Converter and Voltage Source Converter Applications. Thesis for the degree of Doctor of Technology. TUT, Tampere. 169 p.
- [13] T. Ackermann, *Wind Power in Power Systems*. John Wiley & Sons, Ltd, Royal Institute of Technology, Stockholm, Sweden, 2005.
- [14] Molinas, M., Naess, B., Gullvik, W., Undeland, T. Robust Wind Turbine System against Voltage Sag with Induction Generators Interfaced to the Grid by Power Electronics Converters. IEEJ Transaction on Industry Applications. 2006, Vol. 126, No.7, pp. 865 - 871.
- [15] Liserre, M., Blaabjerg, F., Hansen, S., 2005, Design and Control of an LCL-Filter-Based Three-Phase Active Rectifier. IEEE Transaction on Industry Applications, Vol. 41, No. 5, September/October 2005, pp. 1281 - 1291.
- [16] Karshenas, H.R., Saghafi, H. 2006. Performance Investigation of LCL Filters in Grid Connected Converters. Transmission & Distribution Conference and Exposition 2006. IEEE/PES. pp.1 - 6.
- [17] De Leon, F., Semlyen, A., 1993. Time domain modeling of eddy current effects for transformer transients. IEEE Transactions on Power Delivery, Volume 8, Issue 1, January 1993, pp. 271-280.
- [18] Harrison, J.A. *The Essence of Electric Power Systems*. Pearson Education Limited, 1999.